

Validated Automatic Brain Extraction of Head CT Images

John Muschelli^{c,*}, Natalie Ullman^d, Daniel F. Hanley^d, Ciprian M. Crainiceanu^c

^aDepartment of Biostatistics, Bloomberg School of Public Health, Johns Hopkins University, Baltimore, MD, USA

^bDepartment of Neurology, Division of Brain Injury Outcomes, Johns Hopkins Medical Institutions, Baltimore, MD, USA

Abstract

1. Background

Computed Tomography (CT) imaging of the brain is commonly used in diagnostic settings. Although CT scans are primarily used in a clinical setting, they can also be used to answer hypotheses in the research setting. A fundamental processing step in brain imaging is brain extraction, which is the process of separating the brain tissue from all other tissues. Methods for brain extraction in head CT images has been informally proposed, but never formally validated.

2. Aim

To systematically analyze the performance of FSL's brain extraction tool (BET) on head CT images of patients with intracranial hemorrhage by varying its parameters and options after performing CT-specific preprocessing, and quantitatively comparing its results to a manual gold standard.

3. Methods

Nineteen images from 16 patients with intracranial hemorrhage were selected from 13 different MISTIE (Minimally Invasive Surgery plus recombinant-tissue plasminogen activator for Intracerebral Evacuation) stroke trial centers. Each image was thresholded using a 0 – 100 Hounsfield units (HU) range and BET was applied to these images or these images smoothed with a 1mm Gaussian smoother. BET was applied using 1 of 3 fractional intensity (FI) thresholds: 0.01, 0.1, 0.35 and holes in the brain mask produced by BET were filled. For validation purposes, intracranial masks were manually created for all image volumes by expert CT readers. The resulting brain tissue masks were quantitatively compared to the manual segmentations using sensitivity, specificity, accuracy, and the Dice Similarity Index (DSI). Brain extraction across smoothing and FI thresholds were compared using the Wilcoxon signed-rank test.

4. Results

Smoothing images improves brain extraction results using BET for all metrics and irrespective of the FI threshold. Using an FI of 0.01 or 0.1 performed better than 0.35. Thus, all reported results refer only to smoothed data using an FI of 0.01 or 0.1. Using an FI of 0.01 had a higher median sensitivity (0.9921) than an FI of 0.1 (0.9905, $p < 0.001$), lower specificity (0.9979 vs. 0.998; $p < 0.001$), with no difference in accuracy (0.9971 vs. 0.9971; $p = 0.134$) or DSI (0.9894 vs. 0.9896; $p = 0.066$). These measures are all very high indicating that a range of FI values may produce visually indistinguishable brain extractions.

*Principal Corresponding Author

Email addresses: jmusche1@jhu.edu (John Muschelli), nullman1@jhmi.edu (Natalie Ullman), ghanley@jhmi.edu (Daniel F. Hanley), ccrainic@jhsph.edu (Ciprian M. Crainiceanu)

5. Conclusion

BET performs well at brain extraction on thresholded, 1mm smoothed CT images with an FI of 0.01 or 0.1. Smoothing before applying BET is an important step not previously discussed. Analysis code is provided.

Validated Automatic Brain Extraction of Head CT Images

John Muschelli^{c,*}, Natalie Ullman^d, Daniel F. Hanley^d, Ciprian M. Crainiceanu^c

^c*Department of Biostatistics, Bloomberg School of Public Health, Johns Hopkins University, Baltimore, MD, USA*

^d*Department of Neurology, Division of Brain Injury Outcomes, Johns Hopkins Medical Institutions, Baltimore, MD, USA*

Keywords: CT, skull stripping, brain extraction, validation

6. Introduction

X-ray computed tomography (CT) scanning of the brain is widely available and is a commonly used diagnostic tool in clinical settings [1, 2, 3]. Though analysis of CT images is typically done by qualitative visual inspection, detailed quantification of information using neuroimaging tools is of interest. The reason for this interest is that qualitative inspection of CT scans provides limited quantifiable information that can be used in research. A fundamental processing step for producing quantifiable, reproducible information about the brain is to extract the brain from the CT image. This process is called brain extraction or skull stripping. This step is necessary because CT images often contain non-brain human structures (e.g. skull, eyes, skin) or non-human elements (e.g. pillow, medical devices) that are not pertinent to brain research. We propose a validated automated solution to brain extraction in head CT scans using established neuroimaging software.

In magnetic resonance imaging (MRI), brain extraction has been extensively studied and investigated (see Wang et al. [4] for a good overview of methods). While an extensive literature accompanied by software exist for brain MRI scans, the same is not true for brain CT. Inspired by the brain MRI literature and software tools, we have adapted the Brain Extraction Tool (BET) [5], a function of the FSL [6] neuroimaging software (v5.0.4), to automatically extract the brain from a CT scan. Variations of this pipeline have been presented before in Solomon et al. [7], and have been replicated in more detail in Rorden et al. [8]. Neither presented a formal validation against a set of manually segmented brain images, which is the goal of our study.

7. Methods

7.1. Participants and CT data

We used CT images patients enrolled in the MISTIE (Minimally Invasive Surgery plus recombinant-tissue plasminogen activator for Intracerebral Evacuation) and ICES (Intraoperative CT-Guided Endoscopic Surgery) stroke trials. These patients had an intracranial hemorrhage at time of scanning; for inclusion criteria, see Mould et al. [9]. CT data were collected as part of the Johns Hopkins Medicine IRB-approved MISTIE research studies with written consent from participants.

7.2. Imaging Data

The study protocol was executed with minor, but important, differences across the 13 sites. Scans were acquired using Siemens ($N = 9$), GE ($N = 7$), and Philips ($N = 4$) scanners. Gantry tilt was observed in 14 scans. Slice thickness of the image varied within the scan for 2 scans, referred to as variable slice thickness. For example, a scan may have 10 millimeter (mm) slices at the top and bottom of the brain but with 5mm slices in the middle of the brain. Therefore, the scans analyzed had different voxel (volume element) dimensions and image resolution prior to registration to the template. These conditions represent how scans are presented for evaluation in many diagnostic cases.

*Principal Corresponding Author

Email addresses: jmusche1@jhu.edu (John Muschelli), nullman1@jhmi.edu (Natalie Ullman), dhanley@jhmi.edu (Daniel F. Hanley), ccrainic@jhsph.edu (Ciprian M. Crainiceanu)

7.3. Manual and Automated Brain Extraction

We analyzed 19 scans, corresponding to 16 unique patients. Brain tissue was manually segmented as a binary mask from DICOM (Digital Imaging and Communications in Medicine) images using the OsiriX imaging software (OsiriX v.4.1, Pixmeo; Geneva, Switzerland) by one expert reader. CT brain images and the binary mask obtained using manual segmentation were exported from OsiriX to DICOM format.

The image processing pipeline can be seen in Figure 1. Images with gantry tilt were corrected using a customized MATLAB (The Mathworks, Natick, Massachusetts, USA) user-written script (<http://bit.ly/1ltIM8c>). Images were converted to the Neuroimaging Informatics Technology Initiative (NIfTI) data format using `dcm2nii` (2009 version, provided with MRICro [10]). Images were constrained to values -1024 and 3071 HU to remove potential image rescaling errors and artifacts. No interpolation was done for images with a variable slice thickness. Thickness was determined from the first slice converted and was assumed homogeneous throughout the image.

Each image was thresholded a brain tissue range (0-100 HU). In one variant of the pipeline, the data was smoothed using a Gaussian kernel ($\sigma = 1\text{mm}$) and re-thresholded to 0-100 HU; in the other, the data was not smoothed. BET was then applied, varying the fractional intensity (FI) parameter to determine its influence on performance: we used values of 0.35 (as recommended in Rorden et al. [8]), 0.1, 0.01. After BET was applied, we created a brain mask taking values > 0 HU and filled the holes in the mask (using `fslmaths -fillh`).

~~To further illustrate how smoothing affects brain extraction, we present one example case where brain extraction performance with BET was acceptable only after smoothing.~~

7.4. Measuring and Testing Brain Extraction Performance

We compared the masks from above to the manually segmented images. Five common measurements of performance were calculated for each image: sensitivity, specificity, accuracy, and the Dice Similarity Index (DSI). For each measure, higher values indicate better agreement with the manual segmentation. See Inline Supplementary Methods 1 for the calculation of each measure.

~~[Insert Supplementary Methods 1 here]~~

We calculated the paired difference of each measure using different pipelines (e.g. 0.01 vs. 0.1, smoothed data). We tested these differences using the Wilcoxon signed-rank test.

8. Results

Figure 2A illustrates the performance of each variation of the BET pipeline in Figure 1. The smoothed pipelines (top) perform better than the unsmoothed pipelines (bottom) on all measures except specificity (all $p < 0.01$, uncorrected). We also note that BET performs poorly on some scans without smoothing.

Figure 2B displays the performance for brain extraction for the pipelines using smoothed images. Because the performance for all metrics was high when using smooth images, it was necessary to change the y-axis from $[0, 1]$ to $[0.95, 1]$. Using an FI of 0.01 or 0.1 performed better than 0.35; we will focus and compare these results for these values of FI when BET was applied to smooth images. Using an FI of 0.01 had a higher median sensitivity (0.9921) than an FI of 0.1 (0.9905, $p < 0.001$), lower specificity (0.9979 vs. 0.998; $p < 0.001$), and no difference in accuracy (0.9971 vs. 0.9971; $p = 0.134$) or DSI (0.9894 vs. 0.9896; $p = 0.066$). Overall, regardless of p-values, these measures are all high in practice and largely adequate for brain extraction.

Although Figure 2 displays that using FI of 0.01 or 0.1 provides adequate results of brain extraction for most cases, they perform relatively well regardless of smoothing the data. Figure 3 displays an example where using unsmoothed data performs poorly for these FI, demonstrating why smoothing is essential for a general brain extraction procedure for CT. This scan had a high resolution, with voxel size $0.49\text{mm} \times 0.49\text{mm} \times 1$, which may result in more noise in the image, which can reduce performance in BET. Smoothing this image can reduce this noise, which we have seen result in better performance using BET.

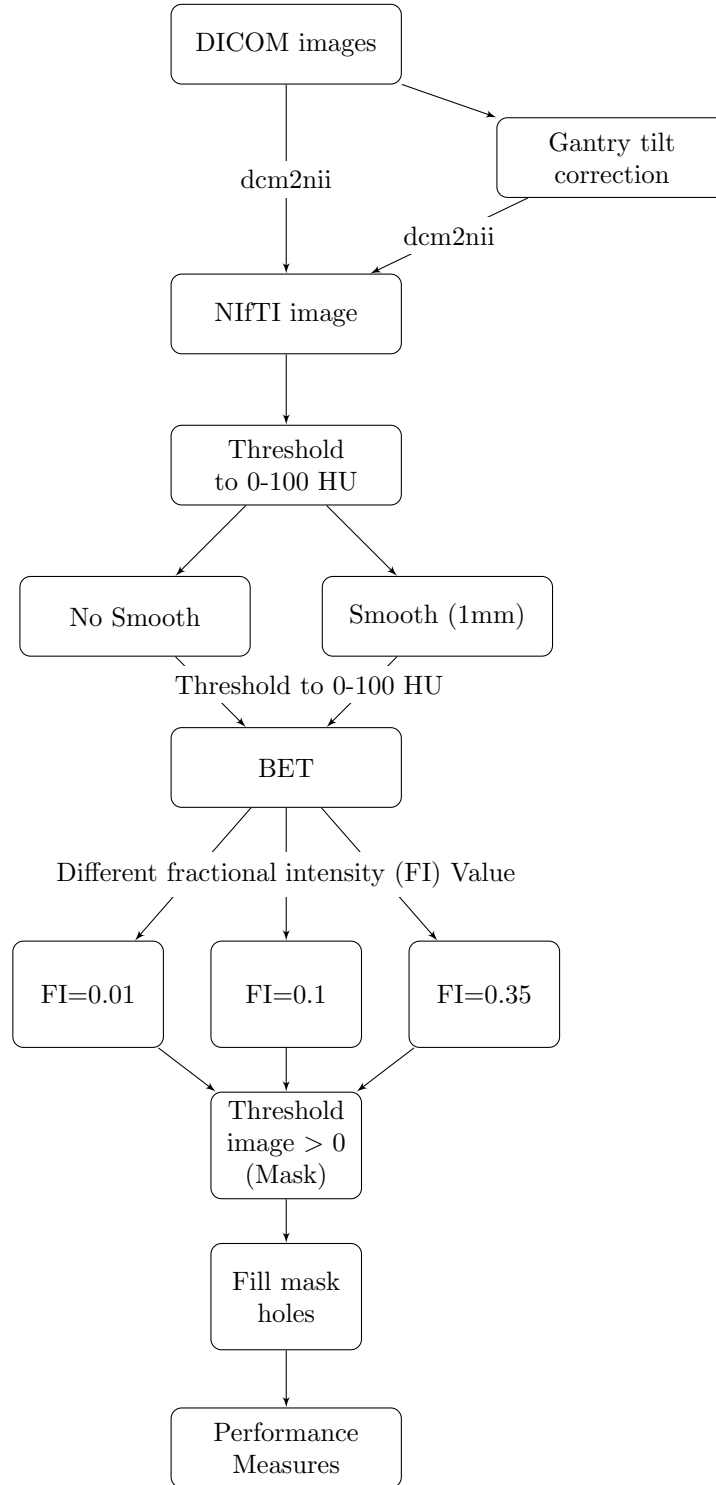


Figure 1: **Processing Pipeline.** Images in DICOM (Digital Imaging and Communications in Medicine) format were gantry tilt corrected if necessary and converted to NIfTI (Neuroimaging Informatics Technology Initiative) format. After NIfTI conversion, the data is thresholded to tissue ranges of 0-100 Hounsfield units (HU). In one variant of the pipeline, the data was smoothed using a Gaussian kernel ($\sigma = 1\text{mm}$); in the other, the data was not smoothed. BET was applied to the image using 3 different fractional intensity (FI) values: 0.01, 0.1, 0.35. The resultant image was masked to values > 0 and FSL was used to fill in any holes. These filled masks were used in comparison to the manually segmented image.

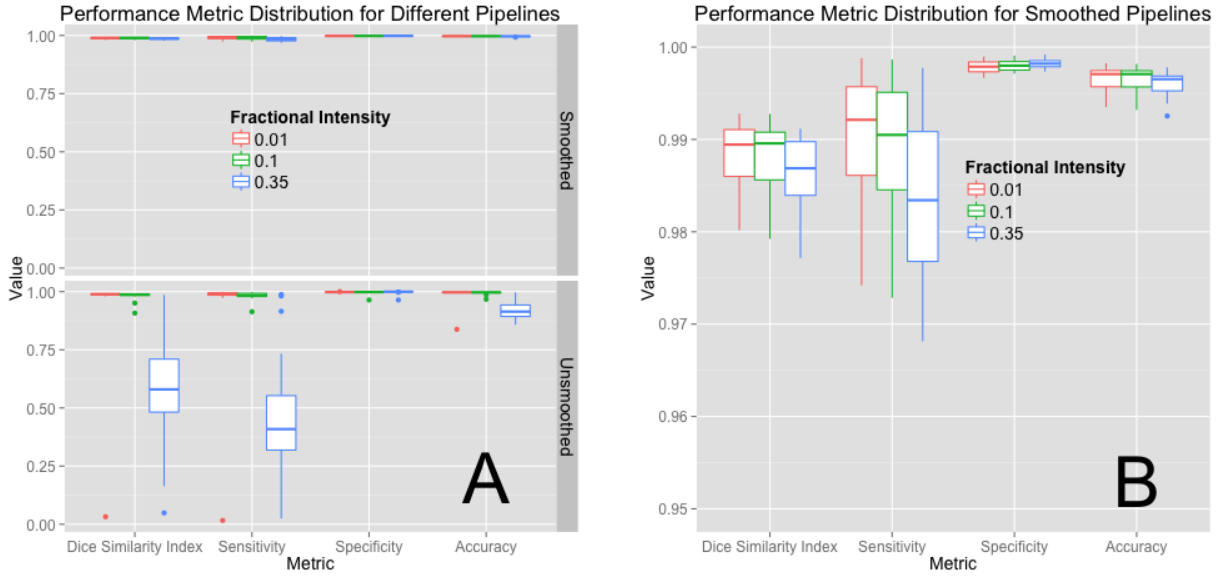


Figure 2: **Performance Metric Distribution for Different Pipelines.** Panel A displays the boxplots for performance measures when running the pipeline with a different fractional intensity (FI), using smoothed data (top) or unsmoothed data (bottom). Panel B presents the smoothed data only, rescaled to show discrimination between the different FI. Overall, FI of 0.01 and 0.1 perform better than 0.35 in all categories other than specificity. Using smoothed data improves performance in all performance metrics, markedly when an FI of 0.35 is used. Panel B demonstrates that using an FI of 0.01 on smoothed data is the best pipeline.

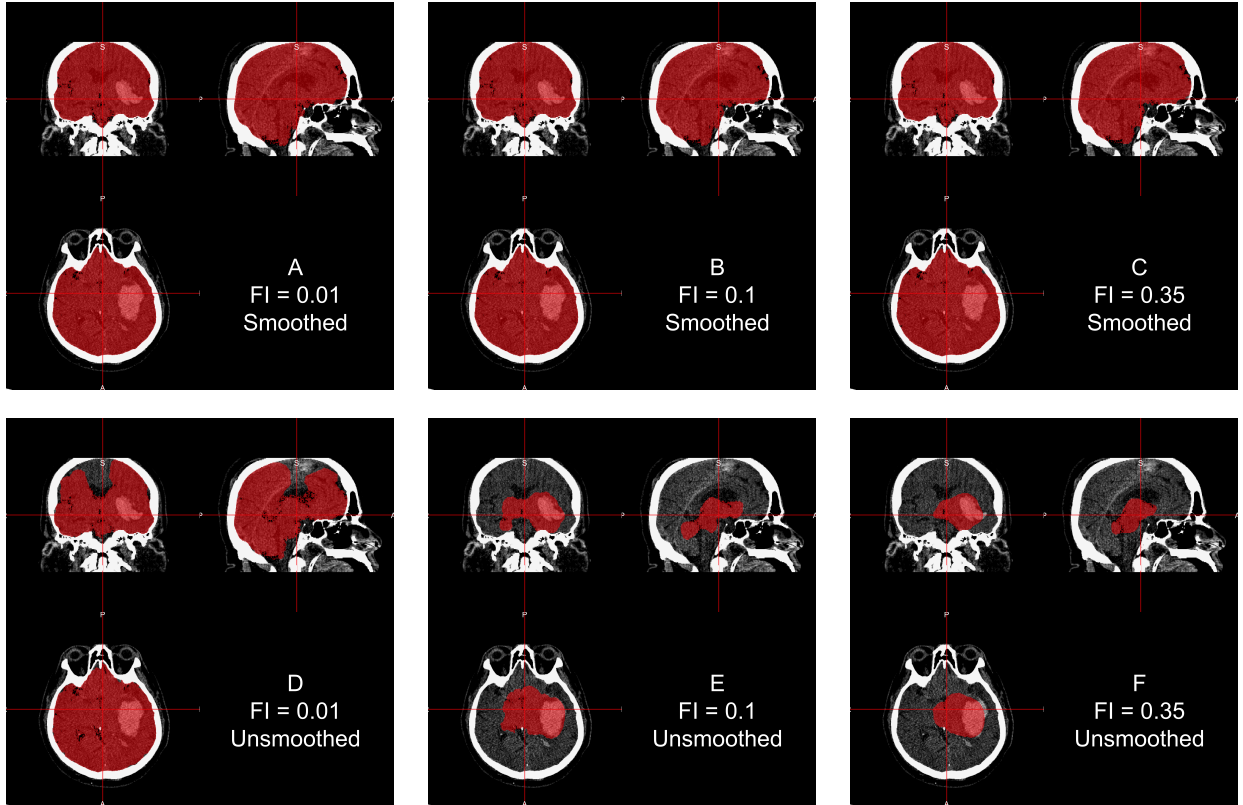


Figure 3: **Example Case where Smoothing before BET is Required** For one subject, the CT image is displayed with the brain extracted mask in red after running all pipelines. Panels A, B, and C represent applying BET using FI of 0.01, 0.01, and 0.35, respectively, to smoothed data. Panels D, E, and F correspond to applying BET using FI 0.01, 0.01, and 0.35 on unsmoothed data. Smoothing images improves brain extraction with BET.

9. Conclusions

Many quantitative procedures of head CT images may require brain-only images for analysis, such as brain volume estimation, intensity normalization, segmentation, and registration. We present an automated brain extraction pipeline for head CT images, which was validated using gold-standard manual segmentations of brain tissues. Overall, we found that smoothing the data with a conservative smoother (1mm Gaussian kernel) and using an FI of 0.01 or 0.1 provides good brain extraction for the sample studied.

We believe this pipeline is generalized for most brain CT scans. Although the sample size is small, the images used are from different people, different centers, and different scanners, which should represent a wide range of scanning parameters. As CT scans have relatively standardized units (Hounsfield units), these parameters should extend to many different settings and the range of values for threshold should be robust.

Moreover, we provide ready-to-use software for CT brain extraction. The R function to perform brain extraction is located at http://bit.ly/CTBET_RCODE and example bash script http://bit.ly/CTBET_BASH. As this software (FSL and R) are free and open-source, our method is readily available to all users.

Acknowledgements

We thank the patients and families who volunteered for this study and Genentech Inc. for the donation of the study drug (Alteplase).

Sources of Funding

The project described was supported by the NIH grant RO1EB012547 from the National Institute of Biomedical Imaging And Bioengineering, T32AG000247 from the National Institute on Aging, R01NS046309, RO1NS060910, RO1NS085211, R01NS046309, U01NS080824 and U01NS062851 from the National Institute of Neurological Disorders and Stroke, and RO1MH095836 from the National Institute of Mental Health. Minimally Invasive Surgery and rt-PA in ICH Evacuation Phase II (MISTIE II) was supported by grants R01NS046309 and U01NS062851 awarded to Dr. Daniel Hanley from the National Institutes of Health (NIH)/National Institute of Neurological Disorders and Stroke (NINDS). ICES was led by Co-Principal Investigator Dr. Paul Vespa at the University of California Los Angeles. Minimally Invasive Surgery and rt-PA in ICH Evacuation Phase III (MISTIE III) is supported by the grant U01 NS080824 awarded to Dr. Daniel Hanley from the National Institutes of Health (NIH)/National Institute of Neurological Disorders and Stroke (NINDS). Clot Lysis: Evaluating Accelerated Resolution of Intraventricular Hemorrhage Phase III (CLEAR III) is supported by the grant U01 NS062851 awarded to Dr. Daniel Hanley from the National Institutes of Health (NIH)/National Institute of Neurological Disorders and Stroke (NINDS).

Inline Supplementary Methods 1

Let I_{ia}, I_{im} be the indicators that voxel i is labeled to be in the brain mask for the automatic and manual masks, respectively.

A voxel i is labeled to be a true positive (TP) when $I_{ia} = 1$ and $I_{im} = 1$, false positive (FP) when $I_{ia} = 1$ and $I_{im} = 0$, false negative (FN) when $I_{ia} = 0$ and $I_{im} = 1$, and true negative (TN) when $I_{ia} = 0$ and $I_{im} = 0$. The number of true positive voxels is defined as:

$$\#TP = \sum_{i=1}^V (I_{ia} \times I_{im})$$

Sensitivity is defined as

$$\frac{\#TP}{\#TP + FN} = \frac{\sum_{i=1}^V (I_{ia} \times I_{im})}{\sum_{i=1}^V I_{im}},$$

specificity is defined as

$$\frac{\#TN}{\#TN + FP} = \frac{\sum_{i=1}^V \{(1 - I_{ia}) \times (1 - I_{im})\}}{\sum_{i=1}^V (1 - I_{im})},$$

overall accuracy is defined as:

$$\frac{\#TN + TP}{\#TN + FN + TP + FP} = \frac{\sum_{i=1}^V [(I_{ia} \times I_{im}) + \{(1 - I_{ia}) \times (1 - I_{im})\}]}{\sum_{i=1}^V I_{ia} + \sum_{i=1}^V I_{im}},$$

and the Dice Similarity Index (DSI) is defined as

$$\frac{2 \times \#TP}{\#TN + FN + TP + FP} = \frac{2 \times \sum_{i=1}^V (I_{ia} \times I_{im})}{\sum_{i=1}^V I_{ia} + \sum_{i=1}^V I_{im}}.$$

References

- [1] R. Sahni, J. Weinberger, Management of intracerebral hemorrhage, *Vascular Health and Risk Management* 3 (5) (2007) 701–709, ISSN 1176-6344, URL <http://www.ncbi.nlm.nih.gov/pmc/articles/PMC2291314/>.
- [2] J. A. Chalela, C. S. Kidwell, L. M. Nentwich, M. Luby, J. A. Butman, A. M. Demchuk, M. D. Hill, N. Patronas, L. Latour, S. Warach, Magnetic resonance imaging and computed tomography in emergency assessment of patients with suspected acute stroke: a prospective comparison, *The Lancet* 369 (9558) (2007) 293–298.
- [3] P. D. Schellinger, O. Jansen, J. B. Fiebach, W. Hacke, K. Sartor, A standardized MRI stroke protocol comparison with CT in hyperacute intracerebral hemorrhage, *Stroke* 30 (4) (1999) 765–768.
- [4] Y. Wang, J. Nie, P.-T. Yap, G. Li, F. Shi, X. Geng, L. Guo, D. Shen, A. D. N. Initiative, et al., Knowledge-guided robust mri brain extraction for diverse large-scale neuroimaging studies on humans and non-human primates, *PloS one* 9 (1) (2014) e77810.
- [5] S. M. Smith, Fast robust automated brain extraction, *Human Brain Mapping* 17 (3) (2002) 143155, ISSN 1097-0193, doi:\bibinfo{doi}{10.1002/hbm.10062}, URL <http://onlinelibrary.wiley.com/doi/10.1002/hbm.10062/abstract>.
- [6] M. Jenkinson, C. F. Beckmann, T. E. J. Behrens, M. W. Woolrich, S. M. Smith, FSL, *NeuroImage* 62 (2) (2012) 782–790, ISSN 1053-8119, doi:\bibinfo{doi}{10.1016/j.neuroimage.2011.09.015}, URL <http://www.sciencedirect.com/science/article/pii/S1053811911010603>.
- [7] J. Solomon, V. Raymont, A. Braun, J. A. Butman, J. Grafman, User-friendly software for the analysis of brain lesions (ABLE), *Computer methods and programs in biomedicine* 86 (3) (2007) 245–254.
- [8] C. Rorden, L. Bonilha, J. Fridriksson, B. Bender, H.-O. Karnath, Age-specific CT and MRI templates for spatial normalization, *NeuroImage* 61 (4) (2012) 957–965, ISSN 1053-8119, doi:\bibinfo{doi}{10.1016/j.neuroimage.2012.03.020}, URL <http://www.sciencedirect.com/science/article/pii/S1053811912002935>.
- [9] W. A. Mould, J. R. Carhuapoma, J. Muschelli, K. Lane, T. C. Morgan, N. A. McBee, A. J. Bistran-Hall, N. L. Ullman, P. Vespa, N. A. Martin, I. Awad, M. Zuccarello, D. F. Hanley, Minimally Invasive Surgery Plus Recombinant Tissue-type Plasminogen Activator for Intracerebral Hemorrhage Evacuation Decreases Perihematoma Edema, *Stroke* 44 (3) (2013) 627–634, ISSN 0039-2499, 1524-4628, doi:\bibinfo{doi}{10.1161/STROKEAHA.111.000411}, URL <http://stroke.ahajournals.org/content/44/3/627>.
- [10] C. Rorden, M. Brett, Stereotaxic Display of Brain Lesions, *Behavioural Neurology* 12 (4) (2000) 191–200, ISSN 0953-4180, doi:\bibinfo{doi}{10.1155/2000/421719}, URL <http://www.hindawi.com/journals/bn/2000/421719/abs/>.